Journal of the European Ceramic Society **16** (1996) 1157–1161

PII:S0955-2219(96)00040-4
0955-2219/96/$15.00 + .00

Characterization of Grain Boundary Phase of a Lead-Based Relaxor by Raman Scattering Spectroscopy

Hideyuki Kanai,[a] Yohachi Yamashita,[a] Masato Kakihana[b] & Masahiro Yoshimura[b]

[a]Research and Development Center, Toshiba Corporation, 1 Toshiba-cho, Saiwai-ku, Kawasaki 210, Japan
[b]Materials and Structures Laboratory, Tokyo Institute of Technology, 4259 Nagatudacho, Midori-ku, Yokohama 227, Japan

(Received 8 January 1996; revised version received 22 January 1996; accepted 30 January 1996)

Abstract

The grain boundary phase of a lead-based relaxor was identified by Raman scattering spectroscopy using standard specimens including PbO, PbO_2, and Pb_3O_4, as well as standard specimens synthesized from the compositions of the grain boundary phase analyzed by a scanning transmission electron microscope. It was revealed that the grain boundary phase contains the PbO phase along with the main perovskite phase in addition to the pyrochlore phase. This result agrees well with the results of X-ray photoelectron spectroscopy studies and strongly supports a previously described degradation mechanism for insulation resistance under humid loading conditions: dissolution of PbO in the grain boundary phase into water is the trigger phenomenon leading to degradation. Copyright © 1996 Elsevier Science Ltd

1 Introduction

Lead-based dielectrics called relaxors are solid solutions of perovskite compounds such as $Pb(Mg_{1/3}Nb_{2/3})O_3$, $Pb(Zn_{1/3}Nb_{2/3})O_3$, and $Pb(Fe_{1/2}Nb_{1/2})O_3$. Yonezawa[1] developed the dielectric ceramics $Pb(Fe_{2/3}W_{1/3})O_3$–$Pb(Fe_{1/2}Nb_{1/2})O_3$ and first used them as a dielectric in MLCs (Multilayer Ceramic Capacitors). Since then, many dielectric compounds for use in MLCs have been reported.[2–4] The interest in relaxors results from their great potential, since they are high dielectric constant materials with sintering temperatures below 1100°C. Such low sintering temperatures allow the use of inexpensive internal electrodes, such as Ag/Pd mixtures or alloy, in the MLC production process.

A previous report by the authors[9] revealed that the reliability of a relaxor under humid loading conditions is a function of the nonstoichiometry of A/B, which is the molar ratio of all the elements at A-sites in the ABO_3 perovskite structure to those at B-sites.[5,6] When A/B is equal to or greater than 1·00, a 2–3 nm-thick secondary phase exists at grain boundaries. Assuming that this secondary phase is soluble in water, the grain boundaries can then dissolve into water. The result is a silver metal path formed by the migration of silver through the partially water-filled grain boundaries from the anode side to the cathode side. Ultimately, the resistance of the dielectric material falls. It has generally been accepted that there exists a continuous or semi-continuous amorphous grain boundary phase (approximately 5–10 nm thick) comprising primarily PbO.[7,8] However, it had not been confirmed that the grain boundary phase is PbO. Therefore, the authors made a successful attempt to identify the lead-based grain boundary phase using X-ray photoelectron spectroscopy (XPS); the grain boundary phase was found to consist mainly of PbO and PbO_2. In this paper, identification of the grain boundary phase is attempted using Raman Scattering Spectroscopy (RSS) as a means of confirming the results of the XPS study. The final objective of successive attempts to identify the grain boundary phase of a lead-based relaxor is to explain why the grain boundary phase is the determinant of reliability.

2 Experimental Procedure

The composition of the relaxor dielectric ceramic used in this experiment was $[(Pb_{0.875}Ba_{0.125})]_A[(Mg_{1/3}Nb_{2/3})_{0.5}(Zn_{1/3}Nb_{2/3})_{0.3}Ti_{0.2}]_BO_3$, where the total molar number of elements occupying the A- and B-sites in the perovskite structure are denoted by A and B, respectively. The temperature coefficient of dielectric constant (K) for this relaxor satisfies the Y5U designation of the Electronic Industries Associations (EIA) standard.[10] In order to ensure

the presence of intergranular fractures — and thus the formation of a grain boundary phase — specimens with A/B = 0·95, 1·00, and 1·05 were prepared. Specimens without a grain boundary phase (A/B = 0·95) exhibiting a transgranular fracture were also produced for comparison.

The raw materials used throughout this experiment were reagent-grade oxides and carbonates. The constituents were weighed, mixed by ball-milling with pure water for 24 hours, and then calcined in a closed alumina crucible at 800°C for two hours. After ball-milling the calcined powder with pure water and drying it, 7 wt% of an aqueous solution of 5 wt% polyvinyl alcohol was added. The result was granulated and pressed into disk pellets 10 mm in diameter and 1·5 mm in height at 100 MPa. After binder burnout at 600°C for 10 minutes, the pellets were fired for two hours in a closed magnesia crucible, at 1050°C for A/B = 1·05, and at 1100°C for A/B = 0·95 and 1·00 to obtain dense specimens. An optimum firing temperature was selected to obtain maximum density.

The valence of lead in the grain boundary phases was determined by Raman scattering spectroscopy (Jobin Yvon - Atagobussan T64000, Longjumeau, France). Spectra activated by an argon ion laser (514·5 nm) were measured between 100 and 1200 cm^{-1}. The beam diameter was 1 μm. The fired specimens were cracked open to obtain the 1–2 nm-thick grain boundary phase on the fractured surfaces of A/B = 1·00 and 1·05. Because specimens with A/B = 0·95 break right through the grains, the Raman spectra reflect the internal state of the grains. After being cracked open, specimens were transferred to the specimen holder of a Raman spectroscope, and spectra from the grain boundary phase were measured. Standard specimens used for identification of Raman spectra were PbO (99·99%, High Purity Chemicals Lab., Ltd), PbO_2 (99·9%, High Purity Chemicals Lab., Ltd), and Pb_3O_4 (99·99%, High Purity Chemicals Lab., Ltd). In addition, the composition of two locations in the grain boundaries of specimens with A/B = 1·05 was analyzed by a scanning transmission electron microscope (STEM) (Table 1). Specimens with these compositions (GB#1 and GB#2) were synthesized in the same manner as described above. GB#1 and GB#2 were sintered at 1000°C, 1050°C, and 1100°C for two hours for identification of Raman spectra from the grain boundary phase.

Table 1. Composition of the grain boundary phase, analyzed by STEM, in specimen with A/B = 1·05 fired at 1050°C for 2 h

	Grain boundary phase		
Component	*GB#1*	*GB#2*	*Inside of grains*
PbO	70·4	66·5	61·7
BaO	4·02	4·91	5·08
Nb_2O_3	16·6	19·4	21·73
ZnO	2·16	2·15	2·29
MgO	2·33	2·23	3·10
TiO_2	4·44	4·88	6·06

3 Results and Discussion

3.1 Identification of the grain boundary phase by RSS

Figure 1 shows Raman spectra from the fractured surfaces of specimens with A/B = 0·95, 1·00, and 1·05. Spectra for each specimen consist of six peaks and they are very similar to each other, with the following features: a small peak at 130 cm^{-1} for the specimen with A/B = 0·95, but a broad peak at 139·8 cm^{-1} for specimens with A/B = 1·00 and 1·05 containing the grain boundary phase; the peak at 268·2 cm^{-1} for A/B = 1·00 and 1·05 is shifted toward low wave number, as compared with that for the specimen with A/B = 0·95. Since there is little difference in spectra from the grain boundary phase and within the grain, we speculate that either the grain boundary phase is similar to the perovskite phase inside the grain or signals from the 1–2 nm-thick grain boundary phase on the grain surfaces were diluted by signals from within the grain due to the Ar laser penetrating further than a few hundred nanometers.

Because STEM analysis has clarified that lead is the main component of the grain boundary phase,[6,11] we investigated whether lead mono-oxide exists in the grain boundary phase by comparison with Raman spectra of standard specimens of PbO, PbO_2, and Pb_3O_4. As shown in Fig. 2, the spectrum of PbO at 140·7 cm^{-1} corresponds to the broad spectrum at 139·8 cm^{-1} for A/B = 1·00 and 1·05, even though the peaks present at smaller wave numbers for PbO_2 and Pb_3O_4 do not correspond. In addition, the peak at 268·2 cm^{-1} for A/B

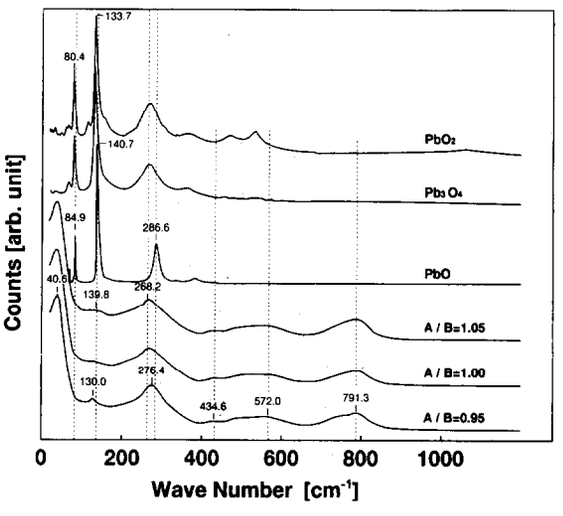

Fig. 1. Raman spectra from fractured surfaces of specimens with (A/B = 1·00 and 1·05) and without (A/B = 0·95) the grain boundary phase as well as reference specimens.

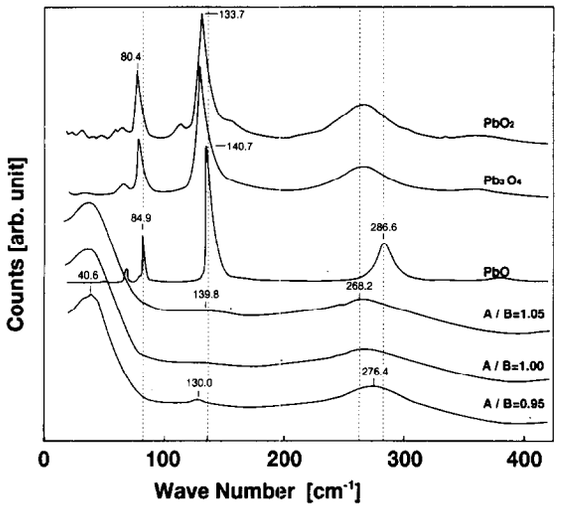

Fig. 2. Detailed view of the low wave number portion of Fig. 1 with an enlarged scale on the horizontal axis.

= 1·05 is broad on the high wave number side, compared to the peak at 276·4 cm^{-1}. Since there is a peak at 286·6 cm^{-1} in the spectrum of the standard specimen of PbO, the spectra for A/B = 1·05 should be convoluted by the interaction of the spectra for the unknown phase and the PbO phase. Moreover, the reason for the slightly broadened peak at 84·9 cm^{-1} for A/B = 1·00 and 1·05 with the grain boundary phase is probably interaction with the spectrum for PbO. Therefore, PbO is not the main constituent of the grain boundary phase, even though the grain boundary phase consists of PbO and an unknown other phase.

In order to identify the grain boundary phase in more detail, grain boundary phases GB#1 and GB#2 were synthesized using the compositions determined by STEM analysis of the grain boundary in the fired specimen with A/B = 1·05. As shown in Fig.3, X-ray diffraction peaks due to the PbO phase, the perovskite phase, and the pyrochlore phase were present in GB#1 and GB#2 fired at 1050°C for two hours. These peaks did not correspond to those for PbO_2 and Pb_3O_4. Since GB#1

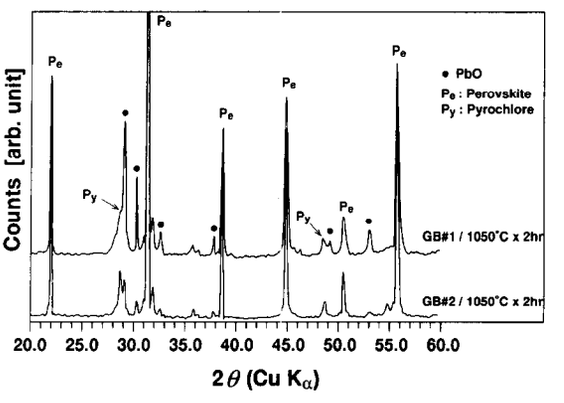

Fig. 3. Powder X-ray diffraction patterns of GB#1 and GB#2 fired at 1050°C for 2 h: GB#1 and GB#2 mainly comprise the perovskite phase in addition to the PbO phase and the pyrochlore phase.

and GB#2 have the compositions given below, the PbO phase and the perovskite phase are expected to be formed in the sintered material.

GB#1:

80 mol%$(Pb_{0.89}Ba_{0.11})[(Mg_{1/3}Nb_{2/3})_{0.44}(Zn_{1/3}Nb_{2/3})_{0.33}Ti_{0.23}]O_3$ + 16 mol% PbO + 4 mol% MgO

or

80 mol%$(Pb_{0.89}Ba_{0.11})[(Mg_{1/3}Nb_{2/3})_{0.71}(Zn_{1/3}Nb_{2/3})_{0.06}Ti_{0.23}]O_3$ + 16 mol% PbO + 4 mol% ZnO

GB#2:

91 mol%$(Pb_{0.89}Ba_{0.11})[(Mg_{1/3}Nb_{2/3})_{0.5}(Zn_{1/3}Nb_{2/3})_{0.28}Ti_{0.22}]O_3$ + 8 mol% PbO + 1 mol% MgO

or

91 mol%$(Pb_{0.89}Ba_{0.11})[(Mg_{1/3}Nb_{2/3})_{0.59}(Zn_{1/3}Nb_{2/3})_{0.19}Ti_{0.22}]O_3$ + 8 mol% PbO + 1 mol% MgO

Raman spectra for GB#1 and GB#2 were measured, as shown in Figs 4 and 5. These spectra are very similar to those for A/B = 1·00 and 1·05 with the grain boundary phase. Three sharp peaks appear at 84·9, 140·7, and 286·6, and these correspond to the peaks for PbO. In addition, since GB#1 and

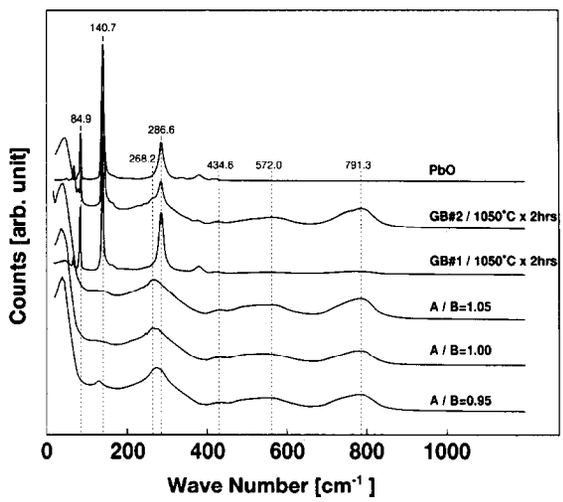

Fig. 4. Raman spectra from fractured surfaces of specimens (GB#1 and GB#2) fired at 1050°C for 2 h.

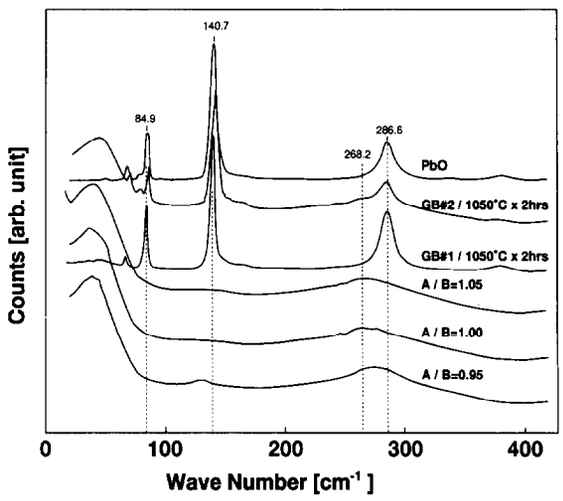

Fig. 5. Detailed view of the low wave number portion of Fig. 4 with an enlarged scale on the horizontal axis.

GB#2 comprise the PbO phase, the perovskite phase, and the pyrochlore phase according to the X-ray diffraction analysis, the remaining broad peaks reflect the perovskite phase and the pyrochlore phase. In Figs 4 and 5, spectra indicating the perovskite phase and the pyrochlore phase in GB#1 and GB#2 correspond to broad spectra for A/B = 1·00 and 1·05 with the grain boundary phase. This confirms that the unknown phases in the grain boundary are the perovskite phase and the pyrochlore phase.

The peak at 268·2 cm^{-1} for A/B = 1·00 and 1·05 with the grain boundary phase is present at slightly lower wave number than that for A/B = 0·95 without the grain boundary phase. In A/B = 0·95, oxygen vacancies may be created to compensate for defects at the A-site in the perovskite, causing binding length shortening. As a result, the wave number increases. In specimens with A/B less than 1.00, the deficiency at the A-site is compensated for the formation of the pyrochlore phase. This result indicates the existence of defects at the A-site in the perovskite structure as well as the formation of the pyrochlore. One reason for peaks for the perovskite phase being broader than those for the PbO phase is that the perovskite phase consists of multiple components, resulting in the existence of multi-vibrational modes. This is in addition to the mixing of the pyrochlore phase into the perovskite phase.

We conclude that the grain boundary phase comprises the PbO phase, the perovskite phase, and the pyrochlore phase. This conclusion strongly supports the degradation mechanism previously presented by the authors.[6] According to this mechanism, the grain boundary phase first dissolves into water and then the grain boundaries fill with water. This leads to Ag migration from the Ag electrode. Thus, PbO peaks in GB#1 would be lower for GB#1 held in water. Change in PbO peaks fractured surfaces of GB#1 fired at 1050°C was investigated by RSS after keeping the fractured specimens in hot water at 85°C for various times. As shown in Fig. 6, the main peak at 140·7 cm^{-1} for PbO started to decrease after 20 hours, and then the peak completely disappeared after 50 hours. A small peak can still be seen after 140 hours, maybe due to distribution of thickness of the grain boundary phase. Thus, it is confirmed that PbO in the grain boundary phase can dissolve in water, suggesting justification of our degradation mechanism for insulation resistance.

3.2 Electrical properties of the grain boundary phase

Figure 7 shows the temperature dependence of the dielectric constant of GB#1. The maximum dielectric constant is 5000 for 1000°C firing and 6500

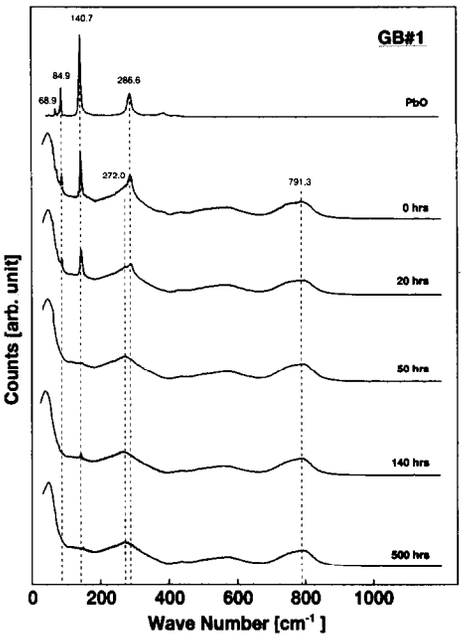

Fig. 6. Raman spectra from fractured surfaces of GB#1 treated in hot water at 85°C for various times.

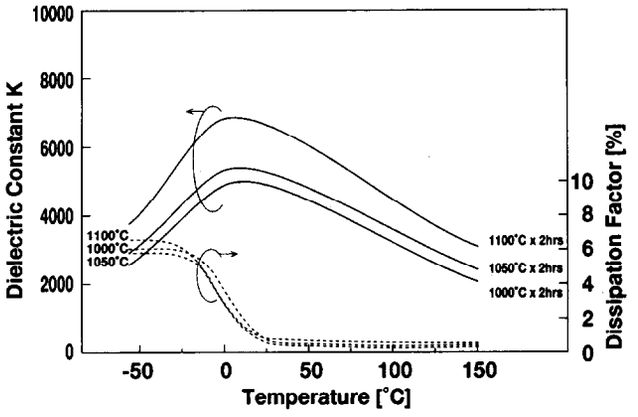

Fig. 7. Dielectric constant and dissipation factor of GB#1 at 1 kHz as a function of temperature.

for 1100°C firing. A previous study reports that there is a PbO-rich grain boundary phase with a dielectric constant of 26.[11] If a grain boundary phase with the low dielectric constant of 26 is present, the decrease in dielectric constant of the bulk specimen would be given as follows, according to the series model:[12] (2 nm-diameter grain with dielectric constant of 12 500)-(2 nm-thick grain boundary phase)-(2 nm diameter grain with dielectric constant of 12 500)

$$C/C_0 = k_2 d_1/(K_2 d_1 + K_1 d_2)$$

where K_1 is the dielectric constant (12 500) of the grain, d_1 is the grain diameter (2 μm), K_2 is the dielectric constant (26) of the grain boundary phase, and d_2 is the thickness (2 nm) of the grain boundary phase. This equation tells us that the dielectric constant decreases by 33% if the dielectric constant of the grain boundary phase is 26, and 0·4% for 6000.

Table 2. Electrical properties of GB#1

	Firing temperature (°C)					
	1,000		*1,050*		*1,100*	
	25°C	*125°C*	*25°C*	*125°C*	*25°C*	*125°C*
C[nF]	7·634	3·961	7·867	4·348	9·033	5·034
DF[%]	0·86	0·27	0·68	0·33	0·85	0·50
IR[Ω]	$0{\cdot}42 \times 10^5$	$0{\cdot}42 \times 10^5$	$0{\cdot}28 \times 10^5$	$0{\cdot}27 \times 10^5$	$0{\cdot}27 \times 10^5$	$0{\cdot}27 \times 10^5$
CR[ΩF]	320	170	190	120	360	210

In a previous study,[12] we reported that the dielectric constant when A/B ≥ 1·01 did not greatly decrease in spite of the existence of the grain boundary phase. This is how we conclude that the main component of the grain boundary phase is not PbO nor the pyrochlore phase with a low dielectric constant, but rather the perovskite phase. This conclusion supports the results of grain boundary phase identification by Raman scattering spectroscopy. Table 2 shows the product of capacitance and resistance (CR) after 1 min at 25°C and 125°C. Independent of firing temperatures CR values at 25°C were 200–400 [ΩF] and at 125°C were 100–200 [ΩF]. These values are considerably lower than those for bulk specimens;[5] that is, they are much less than 10 000 [ΩF] at 25°C and 125°C. If the grain boundary phase is continuously present, the total resistance of bulk specimens should suffer from the effect of the low-resistance grain boundary phase. However, this was not the case. Since the CR value is greater than 10 000 [ΩF] both at 25°C and 125°C,[5] this result suggests that the grain boundary phase is not present continuously in the grain boundaries.

4 Conclusions

It has been clarified that the grain boundary phase of a relaxor dielectric ceramic contains the PbO phase along with the main perovskite phase in addition to the pyrochlore phase. This conclusion strongly supports our degradation model for insulation resistance under humid loading conditions;[6] the insulation resistance degradation in relaxor dielectric ceramics with A/B ≥ 1.00 under humid loading conditions is attributed to dissolution of PbO in the grain boundary phase into water. In addition, the reason for the dielectric constant of specimens with A/B ≥ 1.00 and the grain boundary phase not falling decrease greatly was also elucidated.

Acknowledgement

We would like to thank Mr M. Osada of Tokyo Institute of Technology for carrying out Raman scattering spectrum measurements.

References

1. Yonezawa, M. *et al.*, Properties of $Pb(Fe_{2/3}W_{1/3})O_3$-$Pb(Fe_{1/2}Nb_{1/2})O_3$ Ceramics. *Proc. 1st meeting on ferroelectrics and their application* (1977) 297–302.
2. Maher, G. H., Improved dielectrics for multilayer ceramic capacitors. *Proc. Electro Components Conf.*, **27** (1977) 391–9.
3. Furukawa, K. *et al.*, Dielectric properties of $Pb(Mg_{1/3}Nb_{2/3})O_3$-$PbTiO_3$ ceramics for capacitor materials. *Proc. Japan-US Study Seminar on Dielectrics and Piezoelectric Ceramics* (1982) p. T–4.
4. Kato J. *et al.*, "Dielectric properties of $Pb(Mg_{1/3}Nb_{2/3})O_3$-$Pb(Ni_{1/2}W_{1/2})O_3$ ceramics. *Jpn J. Appl. Phys.*, **24** (1985) suppl. 24-3, p. 90.
5. Kanai, H., Furukawa, O., Nakamura, S. & Yamashita, Y., Effect of stoichiometry on the dielectric properties and the life performance of $(Pb_{0.875}Ba_{0.125})[(Mg_{1/3}Nb_{2/3})_{0.5}(Zn_{1/3}Nb_{2/3})_{0.3}Ti_{0.2}]O_3$ relaxor dielectric ceramics: Part I, Dielectric properties. *J. Am. Ceram. Soc.*, **76** (1993) 454–8.
6. Kanai, H., Furukawa, O., Nakamura, S. & Yamashita, Y., Effect of stoichiometry on the dielectric properties and the life performance of $(Pb_{0.875}Ba_{0.125})[(Mg_{1/3}Nb_{2/3})_{0.5}(Zn_{1/3}Nb_{2/3})_{0.3}Ti_{0.2}]O_3$ relaxor dielectric ceramics: Part II, Life performance. *J. Am. Ceram. Soc.*, **76** (1993) 459–64.
7. Goo, E. & Thomas, G., Microstructure of lead-magnesium niobate ceramics. *J. Am. Ceram. Soc.*, **69** (1986) C-188–C-190.
8. Gorton, A. J. & Chen J., Microstructure and properties of PMN ceramics — influence of powder purity. *Proc. Sixth IEEE Intl Symp. Appl. Ferroelectrics* (1986) 150–3.
9. Kanai, H., Yoshiki, M., Hayashi, M. & Yamashita, Y., Grain boundary phase identification of relaxor dielectric ceramics by XPS. *J. Am. Ceram. Soc.*, 77 (1994) 2229–31.
10. Furukawa, O., Harata, M., Yamashita, Y., Inagaki, K. & Mukaeda, S., A lead perovskite Y5U dielectric for multilayer ceramic capacitor. *J. Appl. Phys. Suppl.*, **26** (1987) 34–7.
11. Hui-Chieh Wang & Schulze, W. A. The role of excess magnesium oxide or lead oxide in determining the microstructure and properties of lead magnesium niobate. *J. Am. Ceram. Soc.*, **73** (1990) 825–32.
12. Payne, D. A. & Cross, L. E., *Proc. Sixth International Materials Symposium, Ceramic Microstructure '76*, ed. R. M. Fulrath & J. A. Pask (1976) 584–97.